

Proceeding Paper

# Development of Graphene-Doped TiO<sub>2</sub>-Nanotube Array-Based MIM-Structured Sensors and Its Application for Methanol Sensing at Room Temperature †

Teena Gakhar \*  and Arnab Hazra 

Department of Electrical and Electronics Engineering, Birla Institute of Technology and Science BITS, Pilani 333031, India; arnabhazra2013@gmail.com

\* Correspondence: gakharteena16@gmail.com

† Presented at the 1st International Electronic Conference on Chemical Sensors and Analytical Chemistry, 1–15 July 2021; Available online: <https://csac2021.sciforum.net/>.

**Abstract:** This work concerns the development of a good quality graphene doped TiO<sub>2</sub> nanotube array sensor for efficient detection of methanol. A pure and graphene doped TiO<sub>2</sub> nanotube array was synthesized by electrochemical anodization. Morphological, structural and optical characterizations were performed to study the samples. Both the nanotube samples were produced in Au/TiO<sub>2</sub> nanotube/Ti type MIM-structured devices. Pure and graphene-doped TiO<sub>2</sub> nanotubes offered a response magnitude of 20% and 28% to 100 ppm of methanol at room temperature, respectively. Response/Recovery time was fast for the graphene doped TiO<sub>2</sub> nanotube array (34 s/40 s) compared to a pure TiO<sub>2</sub> nanotube array (116 s/576 s) at room temperature. This study confirmed the notable enhancement in methanol sensing due to the formation of local heterojunctions between graphene and TiO<sub>2</sub> in the hybrid sample.

**Keywords:** methanol sensing; graphene doping; electrochemical anodization



**Citation:** Gakhar, T.; Hazra, A. Development of Graphene-Doped TiO<sub>2</sub>-Nanotube Array-Based MIM-Structured Sensors and Its Application for Methanol Sensing at Room Temperature. *Chem. Proc.* **2021**, *5*, 74. <https://doi.org/10.3390/CSAC2021-10620>

Academic Editor: Ye Zhou

Published: 6 July 2021

**Publisher's Note:** MDPI stays neutral with regard to jurisdictional claims in published maps and institutional affiliations.



**Copyright:** © 2021 by the authors. Licensee MDPI, Basel, Switzerland. This article is an open access article distributed under the terms and conditions of the Creative Commons Attribution (CC BY) license (<https://creativecommons.org/licenses/by/4.0/>).

## 1. Introduction

Methanol is one of the essential organic solvents having numerous applications in the production of dyes, drugs, perfumes and colors. Moreover, it is extensively utilized in automobile fuel, wastewater denitrification and electricity generation [1]. Methanol is an extremely toxic VOC which is disastrous to human health. Repeated exposure to methanol vapors causes many problems to human beings, such as blindness, acidosis, headaches, blurred vision, shortness of breath and dizziness. Skin contact with methanol results in dermatitis or scaling and eye contact results in vision destruction [2]. With all these concerns, there is a high demand for the development of methanol sensors which are reliable, stable, and sensitive as well as able to perform at low temperatures.

Different materials like metal oxide semiconductors, polymers, carbon nanostructures, metal nanoparticles, and nanocomposites have been extensively utilized by different researchers for chemical sensing. Solid state sensors based on semiconducting metal oxides have achieved a lot in the field of chemical sensing due to their exceptional properties [3]. TiO<sub>2</sub> is an efficient semiconducting metal oxide which can be synthesized in different nanoforms (nanotubes, nanorods, nanoparticles and nanospheres, etc.) for different applications like photocatalysis [4], chemical sensing [5], and wastewater purification [6]. In the field of vapor sensing, the 1D-TiO<sub>2</sub> nanotube performs very well due to its ideal properties such as uniformity, stability and one dimensional electron flow [7]. Different researchers have applied different techniques such as the formation of TiO<sub>2</sub>-based hybrid to improvise the performance of TiO<sub>2</sub>-based sensors.

Two-dimensional graphene offers advanced opportunities to develop hybrids with amazing electronic catalytic behavior. The flat monolayer of graphene offers unique prop-

erties such as high surface-to-volume ratio, excessive mobility and good electrical conductivity [8]. These properties make graphene an ideal candidate to support or form hybrid with metal oxide semiconductors having high catalytic properties [9]. Some reports have been published demonstrating the sensing performance of a graphene-TiO<sub>2</sub>-based hybrid. Fan and group described the hydrothermal production of a TiO<sub>2</sub>-graphene nanocomposite and its implementation in electrochemical sensing. They showed electrochemical sensing of dopamine with excellent sensitivity and selectivity [10]. Ye and co-workers reported room temperature ammonia sensing by an rGO-TiO<sub>2</sub> hybrid. They produced the hybrid by a simple hydrothermal method [11]. Galstyan and group reported the production of an rGO-TiO<sub>2</sub> nanotube hybrid for hydrogen sensing. They showed the impact of GO concentration on the response of TiO<sub>2</sub> nanotubes [12].

In this current work, a highly aligned and uniform graphene-doped TiO<sub>2</sub> nanotube array was synthesized by way of electrochemical anodization for efficient detection of methanol vapors. A pure TiO<sub>2</sub> nanotube array and graphene-doped TiO<sub>2</sub> nanotube array were produced by way of electrochemical anodization. Both samples were examined and analyzed through various characterization techniques which confirmed the presence of graphene in the graphene-doped TiO<sub>2</sub> nanotube array. Metal-insulator-metal (MIM)-structured sensors were produced by using both pure and graphene-doped TiO<sub>2</sub> nanotubes. Graphene-doped TiO<sub>2</sub> nanotubes showed a sensitivity of 28% with quite a fast response and recovery time of 34 s and 40 s towards 100 ppm of methanol. A pure TiO<sub>2</sub> nanotube array, however, showed a sensitivity of 20% with relatively slow response/recovery time (116 s/576 s) in the same conditions.

## 2. Experimental Details

A highly ordered and oriented pure TiO<sub>2</sub> nanotube array and graphene-doped TiO<sub>2</sub> nanotube array were synthesized by electrochemical anodization route. Two-electrode anodic oxidation was performed for 120 min under 40 V potential where Ti foil was used as the anode and graphite was used as the cathode. The electrolyte was made up of 0.5 wt% of NH<sub>4</sub>F, 10% vol of DI water and ethylene glycol. The method to synthesize the TiO<sub>2</sub> nanotube array was described in detail in our previous reports [13].

High purity graphene oxide suspension was used to prepare 0.2 wt% graphene oxide (GO) aqueous solution. Then an electrolyte was prepared with 0.5 wt% NH<sub>4</sub>F, 10 vol% of GO aqueous solution and ethylene glycol for the preparation of a graphene-doped TiO<sub>2</sub> nanotube array. Again, the anodization was performed for 120 min by applying a constant voltage of 40 V. Due to the constant availability of GO in the electrolyte, graphene was doped uniformly in the TiO<sub>2</sub> nanotubes. Both the pure TiO<sub>2</sub> nanotube array and graphene-doped TiO<sub>2</sub> nanotube array were annealed for 3 h at 450 °C in ambient air. Annealing made the nanotubes more robust and stable and hence more reliable to use. The flow chart describing the steps for the synthesis of pure TiO<sub>2</sub> nanotube array and graphene doped TiO<sub>2</sub> nanotube array is represented in Figure 1.

The morphology of the produced samples was analysed by FESEM. The crystallographic structure of both the samples was examined via X-ray diffraction spectroscopy. Raman spectroscopy was performed for both samples which confirmed the doping of graphene in graphene-doped TiO<sub>2</sub> nanotube array (GO-TiO<sub>2</sub>).

To produce the MIM structure for the sensors, Au was deposited on top of TiO<sub>2</sub> nanotube/Ti and GO-TiO<sub>2</sub> nanotube/Ti samples by electron beam evaporation. 100 nm thick deposited Au was considered as the top electrode and Ti was considered as the bottom electrode. Both samples were enveloped in Cu mask to ensure 1\*1mm<sup>2</sup> Au top electrode. A part from the corner of the TiO<sub>2</sub> nanotubes was etched with hydro fluoric acid to induce Ti as the bottom electrode.

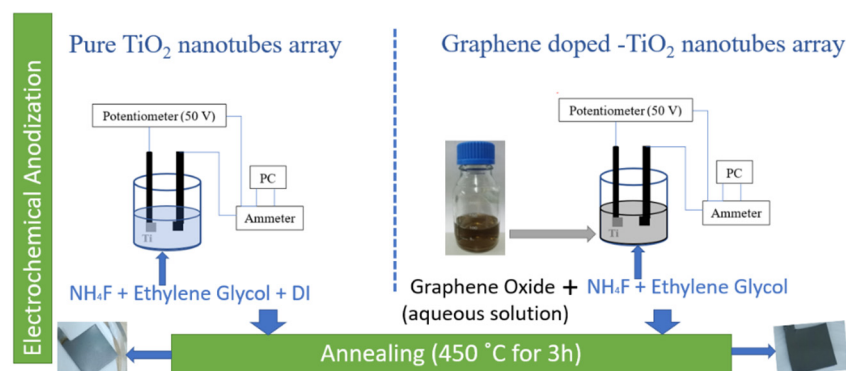


**Figure 1.** Flow chart describing the synthesis procedure of pure TiO<sub>2</sub> nanotube array and graphene-doped TiO<sub>2</sub> nanotube array were synthesized.

The produced sensors were tested against the methanol vapours. The sensors were examined at room temperature. The sensor setup with their properties has been discussed previously [14]. Resistance in the ambient air ( $R_a$ ) and in the exposure of the reducing vapours ( $R_g$ ), methanol was observed. The response magnitude is calculated as  $[(R_a - R_g)/R_a] * 100$ . The response time and recovery time for both sensors is defined as 90% of maximum change of the resistance when exposed to methanol vapours and exposed to synthetic air for the removal of vapors, respectively.

### 3. Results and Discussion

#### 3.1. Material Characterization

FESEM confirmed the formation of highly ordered and uniform nanotubes in both the samples (Figure 2). Highly aligned nanotubes were formed with an approximate average outer diameter of 110 nm and length of 1  $\mu$ m in both the pure TiO<sub>2</sub> nanotube array and graphene doped TiO<sub>2</sub> nanotube array. Graphene does not hamper the original morphology of TiO<sub>2</sub> nanotubes (Figure 2c,d). As graphene was uniformly doped inside the nanotubes, it was hard to observe the graphene with scanning electron microscopy. The chemical composition was studied through the EDS spectra, where the evidence of carbon is clearly visible in a GO-doped TiO<sub>2</sub> nanotube array (Figure 2f).

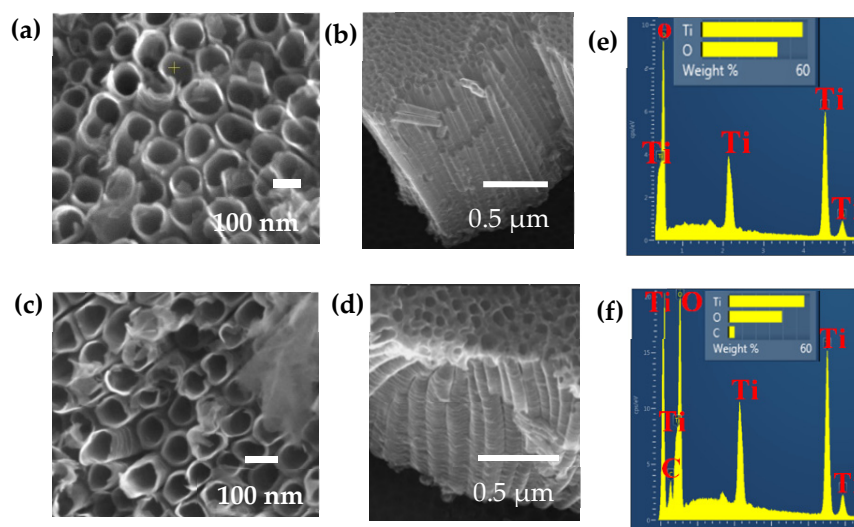


**Figure 2.** FESEM Image of Pure TiO<sub>2</sub> nanotube array (a) Top view, (b) Side view (e) EDS spectra and Graphene-doped TiO<sub>2</sub> nanotube array (c) Top view, (d) Side view (f) EDS spectra.

The sharp intensity peak at  $25.3^\circ$  in both the samples is attributed to the anatase crystallinity of  $\text{TiO}_2$  nanotubes (Figure 3a). A low intensity peak at  $52^\circ$  corresponds to the anatase crystallinity A (105) in both the samples. A small peak at  $54.1^\circ$ , present only in the pure  $\text{TiO}_2$  nanotube array, corresponds to A (201) and clearly shows the presence of more anatase in the pure  $\text{TiO}_2$  nanotube array. The peaks labelled as T arise due to the use of a Titanium substrate in both the samples. T peak intensity is high in the pure  $\text{TiO}_2$  nanotube array and less in the graphene-doped  $\text{TiO}_2$  nanotube array in comparison to the A (101) peak.

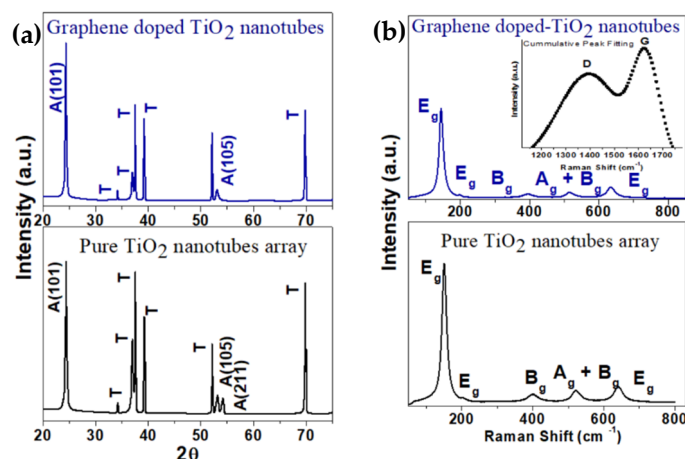


**Figure 3.** Pure  $\text{TiO}_2$  nanotube array and Graphene doped  $\text{TiO}_2$  nanotube array (a) XRD Spectra, (b) Raman spectra.

The Raman spectra of pure  $\text{TiO}_2$  nanotube array and graphene-doped  $\text{TiO}_2$  nanotube array is represented in Figure 3b. The presence of pure anatase is determined by six active modes  $E_g$  ( $144\text{ cm}^{-1}$ ),  $E_g$  ( $197\text{ cm}^{-1}$ ),  $B_g$  ( $399\text{ cm}^{-1}$ ),  $A_g + B_g$  ( $516\text{ cm}^{-1}$ ) and  $E_g$  ( $639\text{ cm}^{-1}$ ) present in both the samples [13]. The sharp intensity peak at  $144\text{ cm}^{-1}$  determines the formation of Ti-O in the anatase phase of  $\text{TiO}_2$ . The presence of graphene is authenticated by the sharp peaks at  $1348\text{ cm}^{-1}$  (D band) and  $1596\text{ cm}^{-1}$  (G band) in the graphene-doped  $\text{TiO}_2$  nanotube array [15]. The active modes of the anatase  $\text{TiO}_2$  nanotube and graphene were present at their corresponding positions even after the uniform doping of graphene.

### 3.2. Methanol Sensing

The two MIM-structure based sensors were examined against the reducing vapours, methanol, at room temperature. The resistance of the pure  $\text{TiO}_2$  nanotube array and graphene-doped  $\text{TiO}_2$  nanotube array was  $90\text{ M}\Omega$  and  $30\text{ M}\Omega$ , respectively. The reduced resistance (increased conductance) of graphene-doped  $\text{TiO}_2$  nanotube array sensor clearly defines the incorporation of graphene inside a  $\text{TiO}_2$  nanotube. Both the sensors were subjected to  $100\text{ ppm}$  of methanol at room temperature. The response magnitude of pure the  $\text{TiO}_2$  nanotube array and graphene-doped  $\text{TiO}_2$  nanotube array was  $20\%$  and  $28\%$ , respectively. The pure  $\text{TiO}_2$  nanotube array had a response time and recovery time of  $116\text{ s}$  and  $576\text{ s}$ , respectively. Moreover, there was the improvement in response time ( $34\text{ s}$ ) and recovery time ( $40\text{ s}$ ) in the case of the graphene-doped  $\text{TiO}_2$  nanotube array (Figure 4a).

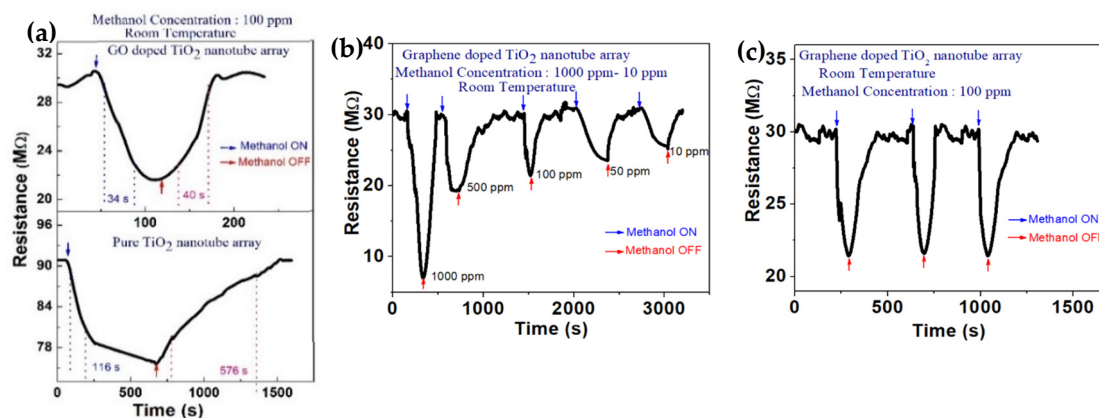


**Figure 4.** (a) Transient behavior of pure TiO<sub>2</sub> nanotube array sensor and graphene-doped TiO<sub>2</sub> nanotube array sensor in 100 ppm methanol at RT with measured response time and recovery time; Graphene-doped TiO<sub>2</sub> nanotube array sensor; (b) Transient behavior from methanol concentration range of: –1000 ppm to 10 ppm; (c) Repeated cycles in 100 ppm methanol at RT.

A transient was measured within a concentration range of 1000 ppm to 10 ppm for a graphene-doped TiO<sub>2</sub> nanotube array sensor (Figure 4b). A good response magnitude was obtained in 1000 ppm methanol (77.7%) and an average response magnitude was obtained in 10 ppm methanol (19%) at room temperature. The graphene-doped TiO<sub>2</sub> nanotube array sensor exhibited a stable baseline resistance with highly repeatable transient behavior at room temperature (Figure 4c). The graphene-doped TiO<sub>2</sub> nanotube array sensor response was improvised with short response time and recovery time due to the incorporation of graphene inside TiO<sub>2</sub> nanotubes.

### 3.3. Methanol Sensing Mechanism

The large surface area and two dimensional structure of graphene enhanced the sensing performance of graphene-doped TiO<sub>2</sub> nanotube array sensor. This increased conductance of graphene doped TiO<sub>2</sub> nanotube array sensor can be attributed to the large carrier mobility and high electrical conductance of graphene. The uniform doping of graphene inside the TiO<sub>2</sub> nanotubes improved the sensing parameters of graphene-doped TiO<sub>2</sub> nanotube array and enabled room temperature sensing.

An energy band diagram of both junctions was sketched by considering the work function of GO  $q\phi_{GO} \sim 4.5$  eV [16] and anatase n-TiO<sub>2</sub>  $q\phi_{TiO_2} \sim 5.1$  eV [17]. An energy band gap of 3.59 eV for pure GO and 3.2 eV for pure TiO<sub>2</sub> (S<sub>0</sub>) were estimated from a literature survey. On the formation of a heterojunction between TiO<sub>2</sub> and GO, electrons are transferred to TiO<sub>2</sub> and get accumulated on the TiO<sub>2</sub> surface.



Surface adsorption of oxygen groups ( $O_2^-$ ,  $O^-$ ,  $O^{2-}$ ) reduces the electron concentration (Equations (1)–(3)) and increases the width of the depletion region, resulting in the formation of built-in potential on the surface of the graphene-doped TiO<sub>2</sub> nanotube array sensor as represented in Figure 5. Upon exposure to the methanol vapors, the trapped electron oxygen groups are released back to the surface of the graphene-doped TiO<sub>2</sub> nanotube array sensor, lowering the built-in potential.





When methanol vapor react with the oxygen species it gets oxidised into formaldehyde, then to formic acid and then it releases electrons to the conduction band which, in turn, reduces the resistance of the sensor in exposure to methanol vapors (Equations (4) and (5)) [18].

Formation of depletion region across the  $\text{TiO}_2$  and GO junction plays an important role for improving the sensor response. Uniform doping of graphene on the  $\text{TiO}_2$  surface is the main reason for enhancing the change of current in-between air and VOC ambient that eventually shows high sensitivity towards methanol by the graphene doped  $\text{TiO}_2$  nanotube sensor at room temperature with quick response time and recovery time.

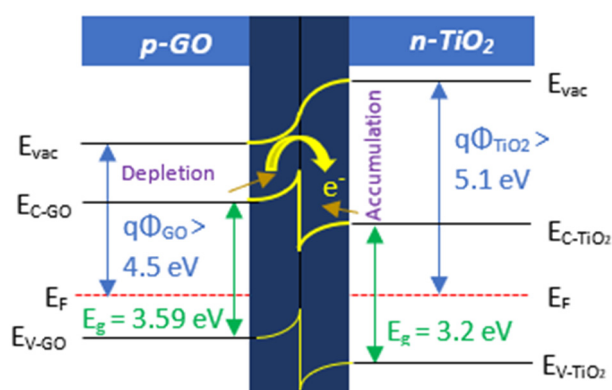


**Figure 5.** Heterojunction formed between *p*-type GO and *n*- $\text{TiO}_2$  nanotubes with electron depletion in GO and electron accumulation in  $\text{TiO}_2$ .

#### 4. Conclusions

In this work, electrochemical anodization was applied to develop pure  $\text{TiO}_2$  nanotube array and graphene-doped  $\text{TiO}_2$  nanotube array. Graphene was doped in the  $\text{TiO}_2$  nanotubes without hampering the original morphology of the nanotubes. Morphological characterization confirmed the formation of highly aligned and uniform nanotubes and structural characterization confirmed the anatase crystallinity of  $\text{TiO}_2$  nanotubes in both the samples. The evidence of graphene in the hybrid nanotubes was authenticated by the D and G peaks in the Raman spectra. The pure and graphene-doped  $\text{TiO}_2$  nanotube array sensor was produced in MIM structure where Au was considered as the top electrode and Ti was considered as the bottom electrode. Pure  $\text{TiO}_2$  nanotube array showed a response magnitude of 20% with slow response time (116 s) and recovery time (576 s) to 100 ppm methanol at room temperature. Graphene-doped  $\text{TiO}_2$  nanotube array showed a better response magnitude of 28% with a quick response time (34 s) and recovery time (40 s) to 100 ppm of methanol at room temperature. Also, lower detection limit till 10 ppm with good response magnitude (19%) towards methanol was achieved with the graphene-doped  $\text{TiO}_2$  nanotube array sensor at room temperature. A significant improvement in methanol sensing was achieved by the formation of localized heterojunctions between graphene and  $\text{TiO}_2$  in the hybrid sample.

**Supplementary Materials:** The following are available online at <https://www.mdpi.com/article/10.3390/CSAC2021-10620/s1>.

**Author Contributions:** Experiment, analysis and writing by T.G.; A.H. designed the research. Review editing and validation was also done by A.H. All authors have read and agreed to the published version of the manuscript.

**Funding:** This work was supported in part by Department of Biotechnology grant (Letter No. BT/PR28727/NNT/28/1569/2018), SPARC grant (SPARC/2018-2019/P1394/SL), and CSIR-SRF Direct (1431120/2k19/1) fellowship Govt. of India.

**Institutional Review Board Statement:** The study was conducted according to the guidelines and Deceleration of BITS Pilani.

**Informed Consent Statement:** Not applicable.

**Data Availability Statement:** Not applicable.

**Conflicts of Interest:** There are no conflicts to declare.

## References

1. Bindra, P.; Hazra, A. Impedance behavior of n-type TiO<sub>2</sub> nanotubes porous layer in reducing vapor ambient. *Vacuum* **2018**, *152*, 78–83. [[CrossRef](#)]
2. Mirzaei, A.; Leonardi, S.G.; Neri, G. Detection of hazardous volatile organic compounds (VOCs) by metal oxide nanostructures-based gas sensors: A review. *Ceram. Int.* **2016**, *42*, 15119–15141. [[CrossRef](#)]
3. Bindra, P.; Gangopadhyay, S.; Hazra, A. Au/TiO<sub>2</sub> Nanotubes/Ti-based solid-state vapor sensor: Efficient sensing in resistive and capacitive modes. *IEEE Trans. Electron. Devices* **2018**, *65*, 1918–1924. [[CrossRef](#)]
4. Zhang, J.; Xu, Q.; Feng, Z.; Li, M.; Li, C. Importance of the relationship between surface phases and photocatalytic activity of TiO<sub>2</sub>. *Angew. Chem.* **2008**, *120*, 1790–1793. [[CrossRef](#)]
5. Liu, Y.; Li, J.; Qiu, X.; Burda, C. Novel TiO<sub>2</sub> nanocatalysts for wastewater purification: Tapping energy from the sun. *Water Sci. Technol.* **2006**, *54*, 47–54. [[CrossRef](#)] [[PubMed](#)]
6. Hazra, A.; Bhowmik, B.; Dutta, K.; Chattopadhyay, P.P.; Bhattacharyya, P. Stoichiometry, length, and wall thickness optimization of TiO<sub>2</sub> nanotube array for efficient alcohol sensing. *ACS Appl. Mater. Interfaces* **2015**, *7*, 9336–9348. [[CrossRef](#)] [[PubMed](#)]
7. Hazra, A.; Bhattacharyya, P. Tailoring of the gas sensing performance of TiO<sub>2</sub> nanotubes by 1-D vertical electron transport technique. *IEEE Trans. Electron. Devices* **2014**, *61*, 3483–3489. [[CrossRef](#)]
8. Geim, A.K.; Novoselov, K.S. *The Rise of Graphene*; Manchester Centre for Mesoscience and Nanotechnology, University of Manchester: Manchester, UK, 2009.
9. Williams, G.; Seger, B.; Kamat, P.V. TiO<sub>2</sub>-graphene nanocomposites. UV-assisted photocatalytic reduction of graphene oxide. *ACS Nano* **2008**, *2*, 1487–1491. [[CrossRef](#)] [[PubMed](#)]
10. Fan, Y.; Lu, H.T.; Liu, J.H.; Yang, C.P.; Jing, Q.S.; Zhang, Y.X.; Yang, X.K.; Huang, K.J. Hydrothermal preparation and electrochemical sensing properties of TiO<sub>2</sub>-graphene nanocomposite. *Colloids Surf. B Biointerfaces* **2011**, *83*, 78–82. [[CrossRef](#)] [[PubMed](#)]
11. Ye, Z.; Tai, H.; Guo, R.; Yuan, Z.; Liu, C.; Su, Y.; Chen, Z.; Jiang, Y. Excellent ammonia sensing performance of gas sensor based on graphene/titanium dioxide hybrid with improved morphology. *Appl. Surf. Sci.* **2017**, *419*, 84–90. [[CrossRef](#)]
12. Galstyan, V.; Ponzoni, A.; Kholmanov, I.; Natile, M.M.; Comini, E.; Nematov, S.; Sberveglieri, G. Reduced graphene oxide-TiO<sub>2</sub> nanotube composite: Comprehensive study for gas-sensing applications. *ACS Appl. Nano Mater.* **2018**, *1*, 7098–7105. [[CrossRef](#)]
13. Gakhar, T.; Hazra, A. Oxygen vacancy modulation of titania nanotubes by cathodic polarization and chemical reduction routes for efficient detection of volatile organic compounds. *Nanoscale* **2020**, *12*, 9082–9093. [[CrossRef](#)] [[PubMed](#)]
14. Bindra, P.; Hazra, A. Selective detection of organic vapors using TiO<sub>2</sub> nanotubes based single sensor at room temperature. *Sens. Actuators B Chem.* **2019**, *290*, 684–690. [[CrossRef](#)]
15. Malard, L.M.; Pimenta, M.A.; Dresselhaus, G.; Dresselhaus, M.S. Raman spectroscopy in graphene. *Phys. Rep.* **2009**, *473*, 51–87. [[CrossRef](#)]
16. Singhal, A.V.; Charaya, H.; Lahiri, I. General synthesis of graphene-supported bicomponent metal monoxides as alternative high-performance Li-ion anodes to binary spinel oxides. *Crit. Rev. Solid State Mater. Sci.* **2017**, *42*, 1–28.
17. Scanlon, D.O.; Dunnill, C.W.; Buckeridge, J.; Shevlin, S.A.; Logsdail, A.J.; Woodley, S.M.; Catlow, C.R.A.; Powell, M.J.; Palgrave, R.G.; Parkin, I.P.; et al. Band alignment of rutile and anatase TiO<sub>2</sub>. *Nat. Mater.* **2013**, *12*, 789. [[CrossRef](#)] [[PubMed](#)]
18. Sahay, P.P.; Nath, R.K. Al-doped ZnO thin films as methanol sensors. *Sens. Actuators B Chem.* **2008**, *134*, 654–659. [[CrossRef](#)]